MECHANISMS OF FATIGUE CRACK GROWTH IN LOW ALLOY STEEL*

R. O. RITCHIE† and J. F. KNOTT†

A study has been made of fatigue crack propagation in a low alloy steel which is subject to temper embrittlement. Effects of mean stress on the growth rate have been examined and comparisons between temper embrittled and unembrittled conditions have been made. Whereas fatigue crack propagation rates were found to be insensitive to mean stress in the unembrittled steel, growth rates in the embrittled condition were significantly faster and were strongly influenced by the level of mean stress.

The effects observed are ascribed to the presence of "static" modes of fracture which occur in association with classical fatigue striations. It is shown that similar static modes can account for effects of mean stress and for the enhanced growth rates observed in a variety of materials of low fracture toughness.

MECANISMES DE CROISSANCE DES FISSURES DE FATIGUE DANS L'ACIER FAIBLEMENT ALLIE

L'étude de la propagation des fissures de fatigue dans un acier faiblement allié soumis à une fragilisation par trempe a été effectuée. L'influence de la contrainte moyenne sur la vitesse de croissance a été examinée et des comparaisons entre les conditions de trempe fragilisantes et non fragilisantes ont été effectuées. Alors que les vitesses de propagation des fissures de fatigue sont insensibles à la contrainte moyenne dans l'acier non fragilisé, les vitesses de croissance dans les conditions fragilisantes sont nettement plus rapides et fortement influencées par le niveau de la contrainte moyenne.

Les effets observés sont attribués à la présence de modes de rupture "statiques" qui se produisent en association avec les formations classiques de stries par fatigue. Les auteurs montrent que des modes statiques analogues peuvent expliquer les effets de la contrainte moyenne et l'augmentation des vitesses de croissance observés dans une variété de matériaux dont la résistance à la rupture est faible.

MECHANISMEN FÜR DAS WACHSTUM VON ERMÜDUNGSRISSEN IN NIEDRIG LEGIERTEM STAHL

Niedrig legierter Stahl wurde einer Temper-Versprödung unterworfen und anschließend die Ausbreitung von Ermüdungsrissen untersucht. Der Einfluß der mittleren Spannung auf die Wachstumsgeschwindigkeit wurde bestimmt und ein Vergleich zwischen nicht getemperten und getemperten Proben durchgeführt. Während die Ausbreitungsgeschwindigkeiten von Ermüdungsrissen im nicht-spröden Material nicht von der mittleren Spannung abhängen, sind die Wachstumsgeschwindigkeiten in den versprödeten Materialien bedeutend größer und hängen stark vom Niveau der mittleren Spannung ab.

Die beobachteten Effekte werden der Gegenwart "statischer" Bruchmoden zugeschrieben, die in Zusammenhang mit klassischen Ermüdungsriefen auftreten. Es wird gezeigt, daß ähnliche statische Moden für Einflüsse der mittleren Spannung und für die in einer Reihe von Materialien mit niedriger Bruchfestigkeit beobachteten höheren Wachstumsgeschwindigkeiten verantwortlich gemacht werden können.

INTRODUCTION

The application of linear elastic fracture mechanics to fatigue crack propagation in metals has led to the formulation of a variety of semi-empirical expressions which relate the crack growth increment per cycle (da/dN) to the stress intensity (K_I) at the crack tip. In general, most of these relationships are based on the original equation presented by Paris,[1] namely:

$$\frac{da}{dN} = C\,\Delta K^m \qquad (1)$$

where 'C' and 'm' are assumed to be material constants and ΔK is the alternating stress intensity, given simply by the difference between the maximum and minimum values for each cycle; i.e. $\Delta K = K_{max} - K_{min}$.

This relationship has been found to represent the behaviour of a large number of materials, and to hold for a wide range of growth rates.[2] It does not hold for very low values of ΔK, where some kind of "threshold" effect appears to exist, nor for very high values of K_{max}, which approach the material's fracture toughness(K_{IC}).[3,4] Values of the exponent 'm', which is the slope of the "crack growth-rate curve" based on equation (1), have been found to lie mainly in the range 2–4, but there is recent evidence that, in medium and high strength steels, much higher values (up to 10) can be obtained, particularly in steels of low fracture toughness.[5–7]

Continuum models of fatigue crack growth are generally based on a mechanism which involves the production of ductile striations, where growth is controlled by the local alternating plastic deformation at the crack tip. A typical model, due to Liu and co-workers,[8–10] predicts that the slope, m, for the mid-range of growth rates, is constant and equal to 2, but this value is merely at the minimum end of the range found experimentally. It seemed plausible to us that the steeper slopes often observed in practice might result from the occurrence of additional modes of fracture during fatigue crack propagation. Effects of

* Received August 4, 1972.
† Department of Metallurgy and Materials Science, University of Cambridge, Pembroke St., Cambridge, CB2 3QZ.

this type have been observed recently in mild steel,[11] and in pearlitic gauge plate.[12]

A further important point is that these additional "static" or monotonic fracture modes during fatigue striation growth might also help to explain why fatigue crack propagation is sensitive to mean stress in some materials, but not in others.[13] Segments of fracture which are strongly dependent on the magnitude of the *maximum* stress intensity at the crack tip, such as cleavage, intergranular cracking or void coalescence, would be promoted by an increase in mean stress, and therefore would be expected to give rise to accelerated fatigue crack growth rates.

To investigate possible effects in the technologically important quenched and tempered steels, we have studied fatigue crack propagation in a medium-strength, low alloy steel which is subject to temper embrittlement. Here, by a suitable heat treatment, it is possible to produce two structures of identical room temperature tensile properties but with markedly different resistances to intergranular brittle cracking in notched tests.

EXPERIMENTAL DETAILS

The material used during this investigation was an arc-melted low alloy steel, En30A, having the composition shown in Table 1, and was supplied in the form of hot-rolled 22 mm square bar. The high hardenability of this steel enables fully martensitic structures to be obtained on air cooling from the austenitizing temperature. Such air-cooling obviates any danger of quench cracking. Studies of the development of temper embrittlement in this steel[14–17] have shown that a fully embrittled structure can be obtained by tempering in the range 450–550°C, where 'tramp' elements, principally antimony,[18] segregate to the prior austenite grain boundaries.

TABLE 1. Composition of low alloy steel *En*30*A*

	C	Ni	Cr	Mo	Si	Mn
wt.%	0.35	4.23	1.43	0.13	0.14	0.44

To obtain the unembrittled and embrittled conditions, all specimens were austenitized for 6 hrs at 950°C and air cooled to produce a fully martensitic structure with a prior austenite grain size of 60 μm. Specimens were then tempered for 1 hr at 650°C. Temper embrittlement, without further softening, was induced in half the specimens by a subsequent isothermal treatment of 8 hrs at 540°C. Typical microstructures of the unembrittled and embrittled steel are shown in Fig. 1. The prior austenite grain boundaries have been delineated by etching in a saturated solution of picric acid containing a few ml of

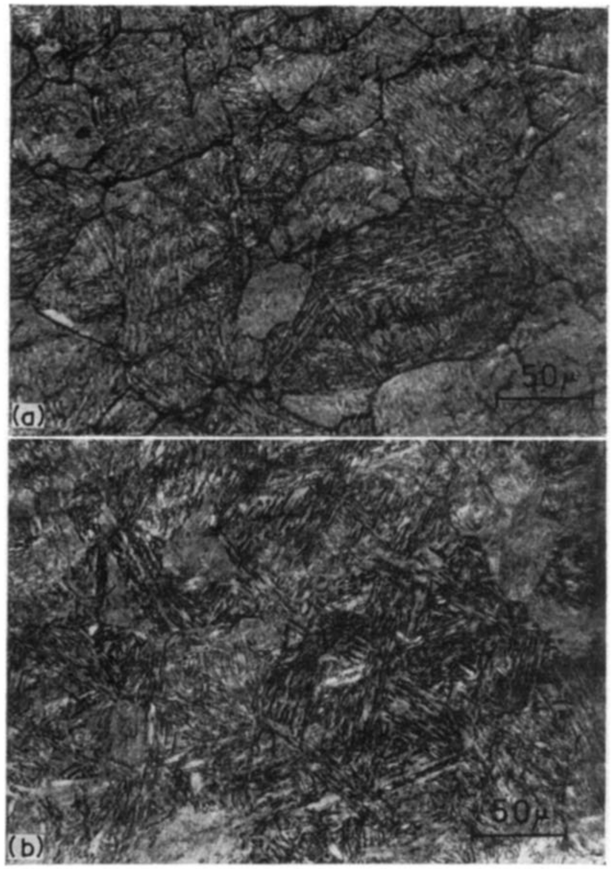

FIG. 1. Typical microstructures of (a) temper embrittled and (b) unembrittled *En*30*A*.

"teepol" (sodium alkyl sulphate) at 75°C. The etch produces a characteristic "grooving" of boundaries where segregation has occurred.[19] A standard two minute etch revealed clear grain boundary "grooving" in the tempered and embrittled condition (Fig. 1a); but the boundaries were only very lightly etched in the tempered and unembrittled condition (Fig. 1b). Further etching in 2% nital was employed to show the martensitic structure.

Single edge notched (SEN) bend testpieces in the form of 20 mm square bars were used for the fatigue tests. These were provided with sharp 45° V-notches of depth 5 mm to give an initial crack-length to width ratio (a_0/W) of 0.25 (Fig. 2). Hounsfield No. 13 tensile specimens were tested to obtain uniaxial tensile data.

Fatigue specimens were deformed in four-point (pure) bending on a 250 kN servo-controlled electro-hydraulic Mand testing machine operating in a closed-loop configuration under load control. Tests were performed at 20 Hz under sinusoidal tension—tension cycling with load control to within $\pm 1\%$. All experiments were carried out in air at room temperature in a constant temperature enclosure (20°C).

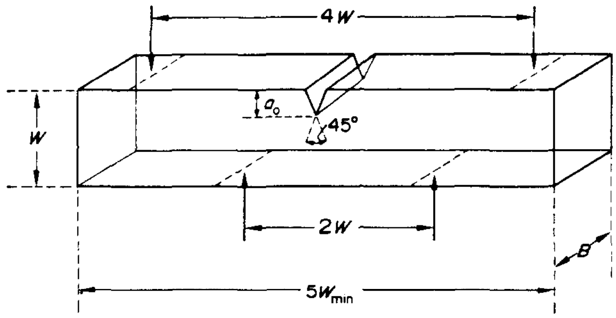

Testpiece dimensions

Thickness B = 20mm
Width W = 20mm
Notch depth a_0 = 5mm

FIG. 2. Geometry of single edge notched bend fatigue testpieces.

In order to determine fatigue crack propagation rates, the crack length a was continuously monitored using the electrical potential method. This entailed passing a constant direct current of 30 A through the testpiece with current stability to 1 part in 10^4. Potential differences generated across the crack were monitored by a cascade of amplifiers with sensitivity to 0.2 μV. Full details of the positioning of the current input and potential monitoring probe positions have been described elsewhere.[20] By employing several experimental calibrations it was found possible to measure crack length to within 0.1 mm, and to detect changes in crack length of the order of 0.01 mm.[21] The experimental data were used initially to construct a graph of crack length versus number of cycles. Growth rates were computed by numerical differentiation of a progression of 'least squares' polynomials fitted to the curves obtained.[21]

The alternating stress intensity (ΔK) at a given crack length was found by determining stress intensity values (K_{max} and K_{min}) corresponding to the maximum and minimum loads of the fatigue cycle. Values of the stress intensity factor (K_I) were computed from these applied loads (P) using the compliance function,[22]

$$K_I = \frac{6M}{BW^{3/2}}\left[1.99\left(\frac{a}{W}\right)^{1/2} - 2.47\left(\frac{a}{W}\right)^{3/2} + 12.97\left(\frac{a}{W}\right)^{5/2} - 23.17\left(\frac{a}{W}\right)^{7/2} + 24.8\left(\frac{a}{W}\right)^{9/2}\right] \quad (2)$$

where W is the width of the testpiece, B its thickness, and 'a' the crack length. M is the applied moment, which in this case is equal to $PW/2$. Equation (2) is considered valid for values of a/W between 0.2 and 0.6. For values of a/W greater than 0.6, a further expression, derived by Wilson,[23] is more appropriate, viz.

$$K_I = \frac{YM}{(W-a)^{3/2}B} \quad (3)$$

where Y is the calibration factor ($Y = 4$ for $(a/W) \geqslant 0.6$).

Corrections to K were applied by considering the size of plastic zone r_y developed at the crack tip, which was estimated from

$$r_y = \frac{1}{\alpha\pi}\left(\frac{\Delta K}{2\sigma_y}\right)^2 \quad (4)$$

where σ_y is the uniaxial yield stress and α is a numerical factor equal to 2 for plane stress, and 6 for plane strain. With the material and applied stresses used in the present investigation the maximum correction for plasticity did not exceed 2 per cent.

The effect of mean stress on fatigue crack propagation was examined by performing tests at a range of stress ratios $R = K_{min}/K_{max}$ ranging from 0.05 to 0.60. In each case the initial alternating stress intensity (ΔK_i) was maintained constant at 15 $MNm^{-3/2}$. The initial stress intensities and applied loads are summarised in Table 2.

TABLE 2. Initial stress intensity and load ranges for fatigue tests

R (K_{min}/K_{max})	ΔK_i $MNm^{-3/2}$	K^i_{max} $MNm^{-3/2}$	K^i_{min} $MNm^{-3/2}$	P_{max} kN	P_{min} kN
0.05	15	15.8	0.8	15.52	0.78
0.40	15	25.0	10.0	24.58	9.79
0.50	15	30.0	15.0	29.49	14.77
0.60	15	37.5	22.5	36.88	22.15

Where R is the stress ratio; ΔK_i, K^i_{max}, K^i_{min} are the initial stress intensities at the start of a test, and P_{max} and P_{min} are the applied loads.

Fracture surfaces were examined optically and in the scanning electron microscope.

RESULTS

The room temperature toughness and tensile properties of the steel, in the unembrittled and embrittled conditions, are shown in Table 3. It can be seen that the embrittling treatment does not alter the tensile properties, but reduces the fracture

TABLE 3. Tensile properties and fracture toughness of *En*30*A* at room temperature

	0.2% Proof Stress MNm^{-2}	U.T.S. MNm^{-2}	Reduction in area	K_{Ic} $MNm^{-3/2}$
unembrittled	743	1014	60%	75
embrittled	735	998	60%	40

toughness by a factor of almost two. Fractography of the fracture toughness testpieces revealed that the unembrittled steel had failed by micro-void coalescence whereas the embrittled steel had fractured entirely by brittle intergranular cracking along the prior austenite grain boundaries (Fig. 3).

The results of the fatigue tests are shown in Fig. 4, in terms of crack length (a) versus number of cycles (N). Lifetimes of specimens in the embrittled condition were in all cases shorter than in corresponding tests in the unembrittled condition. Furthermore, a consistent trend of decreasing lifetime for increasing

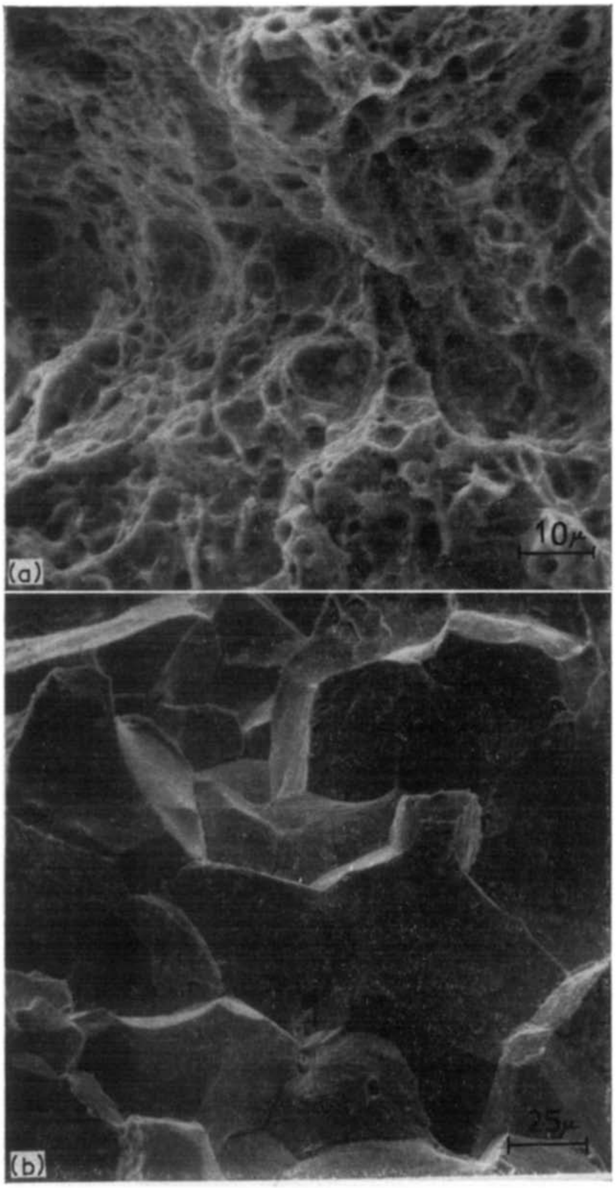

FIG. 3. Final failure of fracture toughness specimens of (a) unembrittled steel by microvoid coalescence; and (b) embrittled steel by brittle intergranuar cracking.

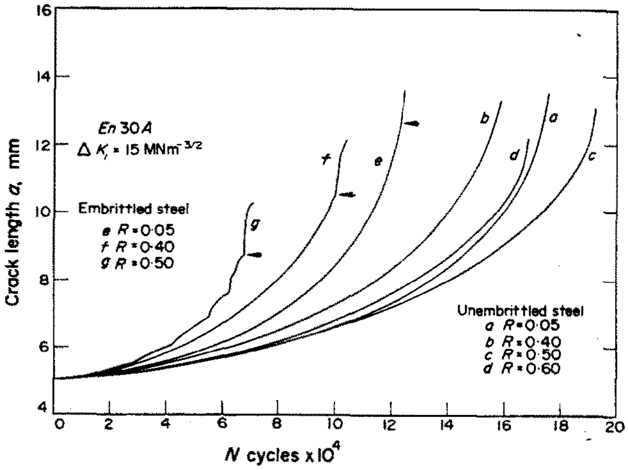

FIG. 4. Curves of crack length versus number of cycles from fatigue tests on unembrittled and embrittled testpieces. Initial alternating stress intensity $\Delta K_i = 15$ MNm$^{-3/2}$.

mean stress (or R value) was observed for the embrittled steel, but was far less apparent in results on the unembrittled material. The crack length curves for the unembrittled condition appear to be relatively smooth. Those for the embrittled steel show marked discontinuities, particularly at high stress levels.

Crack growth rates, plotted in terms of the alternating stress intensity, for the unembrittled and embrittled conditions are shown in Figs. 5 and 6 respectively.

With regard to the unembrittled steel, Fig. 5 confirms the absence of any significant effect of mean

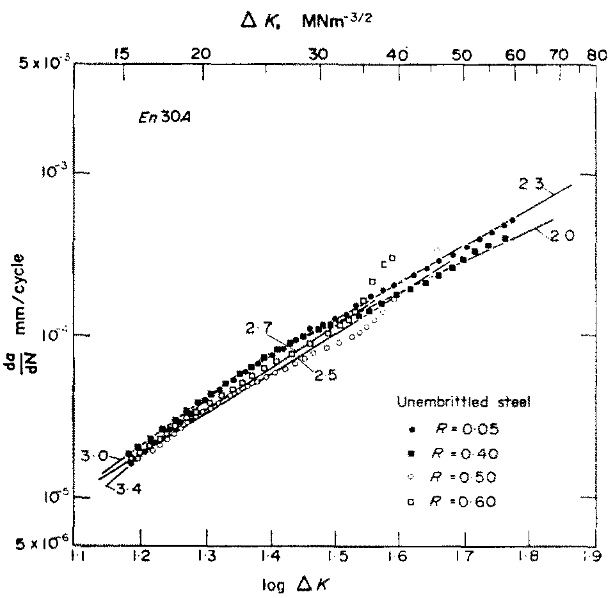

FIG. 5. Variation of crack growth rate (da/dN) with alternating stress intensity (ΔK) for range of stress ratios $R = 0.05$–0.60 for unembrittled steel. (Numbers indicate slopes (m) of regression lines drawn through data points.)

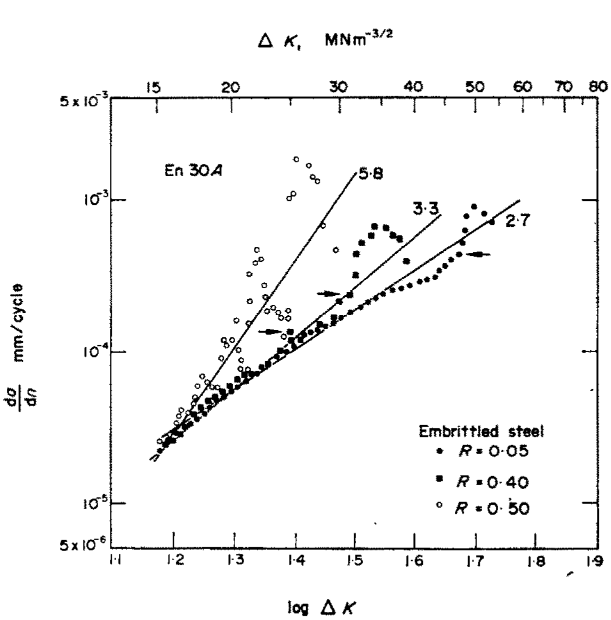

FIG. 6. Variation of crack growth rate (da/dN) with alternating stress intensity (ΔK) for range of stress ratios $R = 0.05$–0.50 for embrittled steel. (Numbers indicate slopes (m) of regression lines drawn through data points.)

stress on the propagation rate; the broad pattern of data falling within a narrow scatterband of slope (m) approximately equal to 2.4. Least squares regression analyses of the individual curves were carried out and showed 'm' to vary between 2.0 and 2.7 for the four values of the stress ratio R.

Scanning electron microscopy of the fracture surfaces revealed that the mechanism for fatigue propagation in the unembrittled steel was by ductile striation growth for all values of R (Fig. 7); well-defined ripples being observed over the majority of the fracture surface.

Small, but significant, increases in the general slopes in Fig. 5 occur at low values of ΔK for the low mean stress tests ($R = 0.05$ and 0.40) and at high values for the high mean stress tests. Associated with the increased slope (≈ 3) at low values of ΔK, isolated intergranular facets were observed on the fracture surface in addition to the normal ductile striations (Fig. 8). These intergranular facets were not observed at stress levels of $K_{max} \geqslant 30$ MNm$^{-3/2}$, and were virtually absent, except at initiation, in the higher mean stress tests. In all cases this failure followed the prior austenite grain boundaries while the ductile striation growth was entirely transgranular through the tempered martensite (Fig. 9). At very high stress intensities, the mode of propagation was found to be predominantly void coalescence and this was particularly marked in tests at $R \geqslant 0.50$ (Fig. 10). This again led to an increase in growth rate and a corresponding deviation from the general slope of $m \simeq 2.4$. The incidence of fibrous growth in the lower mean stress tests was confined to a small region prior to final failure, and little or no increase in propagation rate was observed.

The fatigue crack growth-rate curves for the embrittled steel are shown in Fig. 6, where it can be seen that the effect of mean stress is extremely marked in increasing the crack propagation rate, particularly

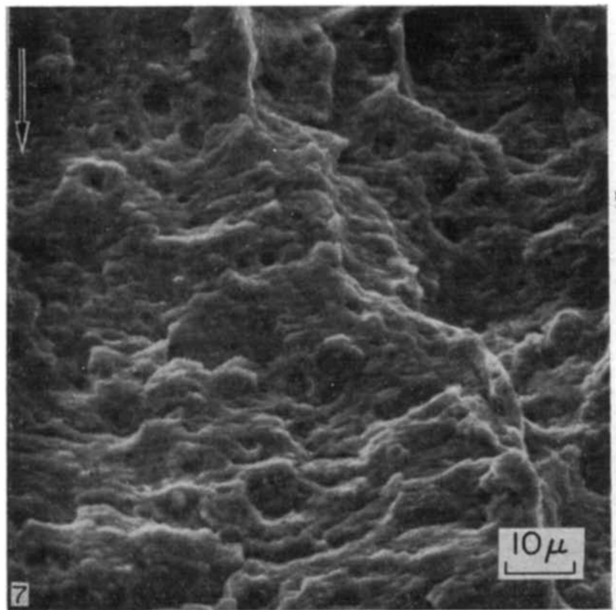

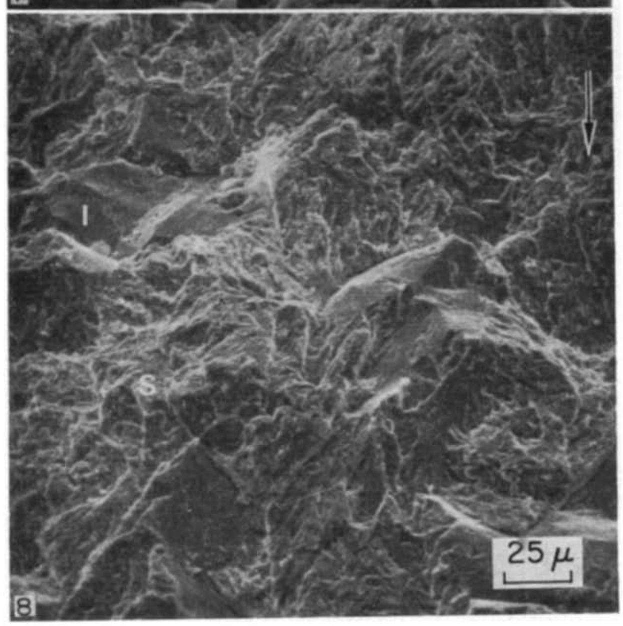

FIG. 7. Ductile striation growth through tempered martensite during fatigue of unembrittled steel. $\Delta K = 45$ MNm$^{-3/2}$, $K_{max} = 47$ MNm$^{-3/2}$ (arrow indicates general direction of fatigue crack propagation).

FIG. 8. Isolated intergranular facets (I) during striation growth (S) in unembrittled steel at low stress intensities. $\Delta K = 15$ MNm$^{-3/2}$, $K_{max} = 16$ MNm$^{-3/2}$.

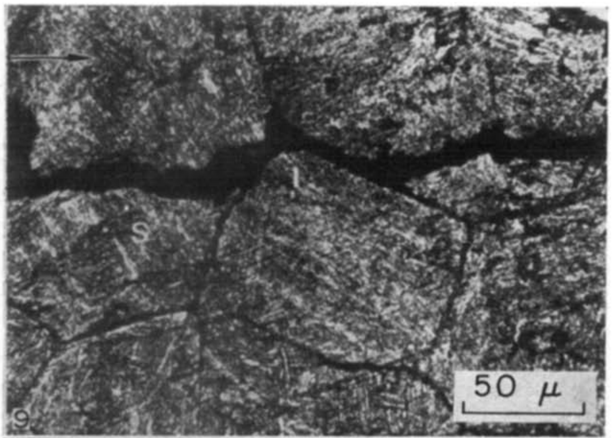

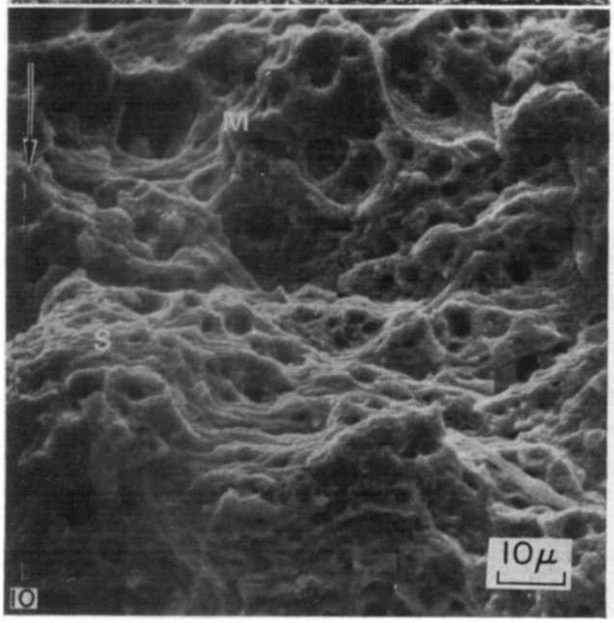

FIG. 9. Section through fatigue growth shown in Fig. 8, showing the transgranular nature of striation growth (S) and the intergranular separation (I) along prior austenite grain boundaries. (Prior austenite grain boundaries delineated by overetching (~20 mins) in hot picric acid.)

FIG. 10. Occurrence of microvoid coalescence (M) and ductile striation growth (S) during fatigue of unembrittled steel in high mean stress tests ($R \geqslant 0.50$) at high values of K_{max}. $\Delta K = 35$ MNm$^{-3/2}$, $K_{max} = 70$ MNm$^{-3/2}$.

at high values of ΔK. The mean slopes (m) of the individual plots, determined from regression analysis, were found to increase from 2.7 for $R = 0.05$ to 5.8 for $R = 0.50$. Furthermore, the data points show many instances of sudden acceleration in growth rate, the frequency and magnitude of these bursts becoming greater in the higher mean stress tests, i.e. for increasing values of K_{max}.

The bursts in growth rate can be identified with bursts of cracking on the fracture surfaces (Fig. 11). Both are entirely absent for unembrittled specimens. For all values of R in the embrittled specimens, a major burst of cracking occurred at a constant critical value of maximum stress intensity (indicated in Table 4 and by arrows in Figs. 4, 6 and 11). Smaller bursts were observed to precede this major event; the number of bursts inceasing with increasing values of R and hence K_{max}. Both these effects suggest that the cracking observed is independent of the *alternating* stress intensity and critically dependent on the *maximum tensile* stress ahead of the crack-tip.

Scanning electron microscopy of the embrittled testpieces showed that at all stress intensities, the total crack growth proceeded by a combination of ductile fatigue striations and intergranular cracking. This cracking was present both as isolated facets (Fig. 12) and as major bursts of fracture (Fig. 13). As for the unembrittled steel, the facets were intergranular with respect to the prior austenite grains, but showed less evidence of plastic deformation and were far more numerous (compare Figs. 8 and 12). Furthermore, this intergranular cracking was observed

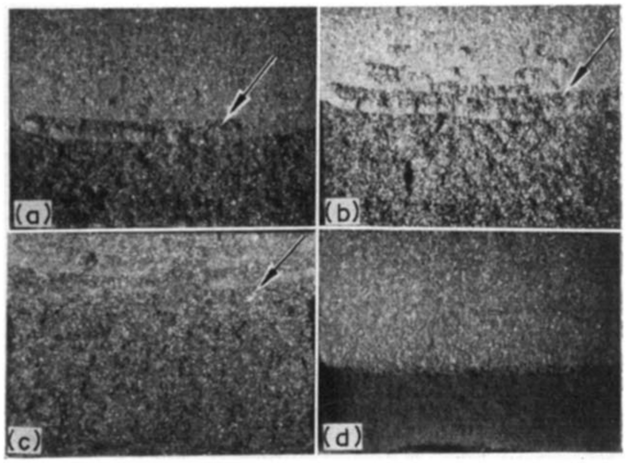

FIG. 11. Final fracture surfaces for embrittled specimens showing onset of major burst of intergranular cracking (marked by arrows), for following stress ratios: (a) $R = 0.05$ (b) $R = 0.40$ (c) $R = 0.50$ (d) $R = 0.40$ in unembrittled material shown for comparison.

TABLE 4. Critical values of stress intensity for onset of major burst in fatigue of embrittled steel

R value (K_{min}/K_{max})	Critical crack length mm	ΔK_{crit} MNm$^{-3/2}$	K_{max}^{crit} MNm$^{-3/2}$
0.05	12.9	49.8	52.0*
0.40	10.4	31.2	51.7
0.50	9.0	25.7	51.2

* It may be noted that the K_{max} values quoted exceed the material's static K_{IC}. This interesting result is entirely consistent with the fact that increasing the K_{max} during prefatiguing of fracture toughness specimens can markedly increase the resulting K_{IC} value.[24]

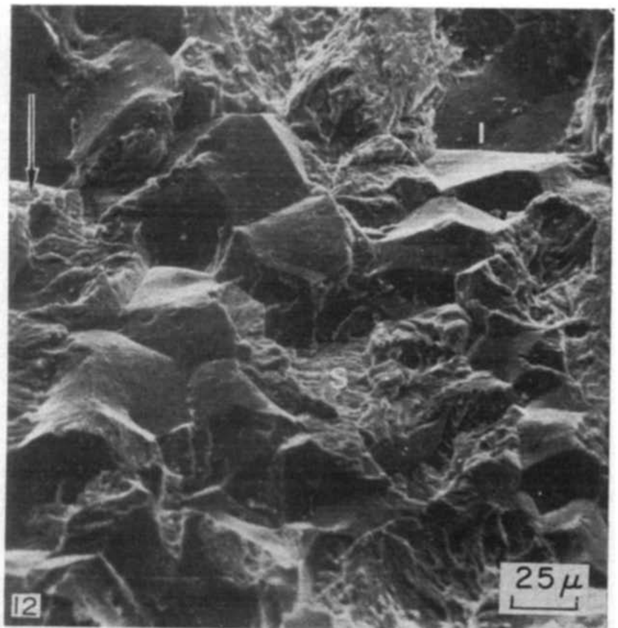

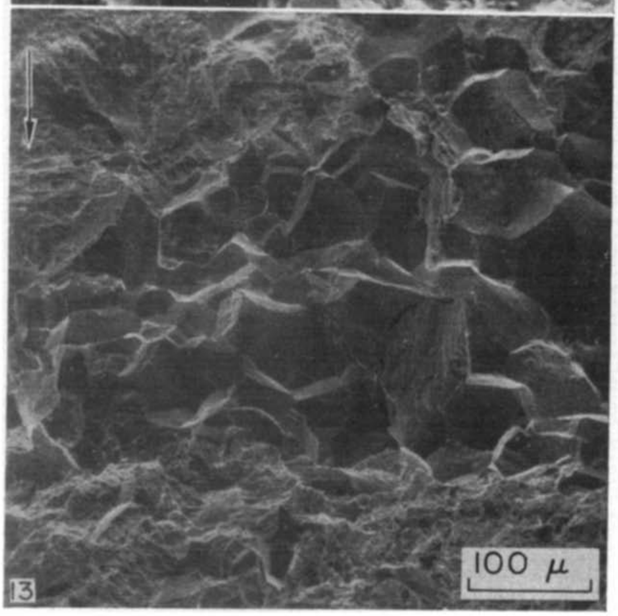

FIG. 12. Brittle intergranular cracking (I) during striation growth (S) in fatigue of embrittled steel. ΔK = 21 $MNm^{-3/2}$, K_{max} = 22 $MNm^{-3/2}$. *Note that this cracking occurs at a value of* K_{max} *less than one half* K_{IC}.

FIG. 13. Burst of brittle intergranular cracking during striation growth in fatigue of embrittled steel. ΔK = 26 $MNm^{-3/2}$, K_{max} = 43 $MNm^{-3/2}$.

throughout the entire range of growth rates, unlike that in the unembrittled steel which was observed only at low values of ΔK.

A comparison of the growth-rate curves and their corresponding slopes (m) for the unembrittled and embrittled steel is summarised in Fig. 14. The principal observation to be made is that the total "fatigue" crack propagation is faster in the embrittled condition, due to the occurrence of intergranular cracking throughout growth. Furthermore, the occurrence, during fatigue, of brittle cracking, which is sensitive to the magnitude of the tensile stress at the crack tip, leads to a situation where the overall crack propagation rate is sensitive to mean stress. When propagation is by the normal ductile striation mechanism, as for the majority of the growth in non-embrittled specimens, little or no such effect is apparent.

DISCUSSION

Such metallurgical mechanisms for fatigue crack growth as exist are based on the concept of one striation growth increment per cycle.[25,26] They have not been applied specifically to growth under linear elastic conditions but would be expected to relate the propagation rate primarily to the *alternating* stress intensity because growth is controlled by the alternating plastic strain per cycle. These mechanisms do not, however, adequately explain any effect of mean stress on the propagation rate. Our results confirm that, where fatigue growth occurs by a ductile striation mechanism, little or no effect of mean stress exists, and the propagation rate is controlled predominantly by ΔK. A similar conclusion has been reached for mild steel.[11,27]

Situations where growth is sensitive to mean stress arise as a consequence of modes of 'static' fracture occurring in addition to the striation mechanism. For example, it has recently been shown that, in mild steel, where propagation normally proceeds by ductile

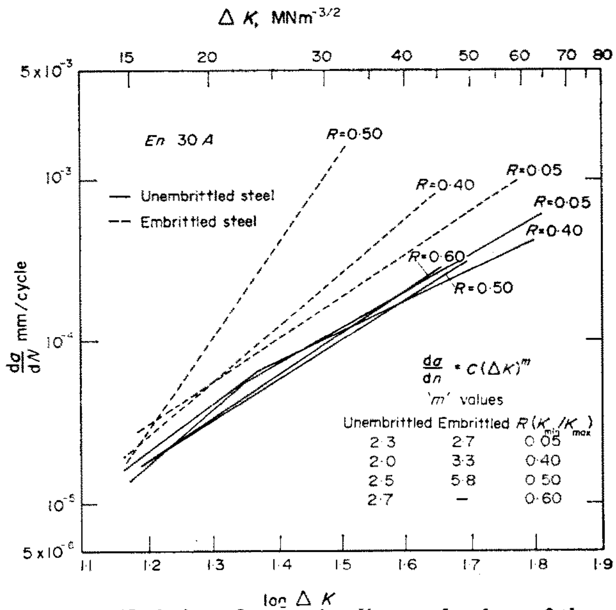

FIG. 14. Variation of regression lines and values of the slope 'm' for the fatigue crack growth rates of unembrittled and embrittled steel at values of stress ratios R studied.

striations and is considered to be insensitive to mean stress,[13] the growth rate becomes markedly dependent on mean stress when 'static' fracture modes occur. Such situations arise when the steel is fatigued below its brittle–ductile transition temperature, when segments of cleavage are observed,[11] or when it is pre-strained, when the propagation may include regions of void coalescence.[28] Further, Griffiths *et al.*[27] have shown that an effect of mean stress is observed in a ferritic weld metal when propagation is accelerated by void coalescence. The results obtianed during the present investigation strongly support this effect of the 'static' fracture component of crack growth. In the embrittled steel, the occurrence of intergranular cracking produced both an increase in growth rate and a dependence of growth rate on mean stress. It is apparent that the onset of such brittle fracture depends critically on the maximum stress produced ahead of the advancing crack tip.

Two consequences of the 'static' fracture component are as follows. Firstly, it is predicted that the mean stress effect is less likely to be observed in thin specimens, because insufficient tensile stress to induce static fracture can be generated if the hydrostatic stress state is small. Evidence for this may be deduced from results obtained for a pearlitic steel[29] and for a high-nitrogen mild steel.[30] Secondly, it would appear that the static component might assume more significance in materials of low fracture toughness because brittle cracks would be relatively more easy to produce. An acceleration of growth rate by increasing mean stress is therefore predicted to occur for materials such as high strength steels, which have low toughness. We have been unable to discover reports of such investigations in the published literature, but would draw attention to the strong effect of mean stress on growth rate in high-strength aluminium alloys possessing fracture toughnesses of the order of 40 $MNm^{-3/2}$ [31,32] In this context, more recent evidence has shown that this strong mean stress effect is absent in aluminium alloys of greater toughness.[33] In these cases, the effect cannot be attributed to gross cracking, but probably involves the brittle cracking of intermetallic particles on a microstructural scale.

The presence of components of 'static' or monotonic fracture during fatigue may also have a strong bearing on the slope of the growth-rate curves, i.e. the exponent 'm' in the Paris relationship [equation (1)]. The results of the present investigation for the embrittled steel at high mean stress show this effect very clearly (Fig. 6). The apparent scatter is a result of the overall growth rate (monitored by potential measurements) being locally accelerated by bursts of cracking. These give rise to an array of data points which, in detail, produce a curve of saw-tooth appearance. Straight lines, derived from regression analysis, have been drawn through these data points, and show an increasing mean total crack growth rate with increasing mean stress. This approach is considered to be justified, since, had the technique for monitoring crack length been of conventional sensitivity (particularly if surface observations only had been made) the local accelerations in growth rate would, in all probability, not have been detected and the saw-tooth character of the resulting array of data points would not have been apparent.

A point made earlier, concerning the effect of mean stress, was that the occurrence of static fracture modes might be more important in materials of low fracture toughness. We have now shown that such segments of fracture can lead to apparent increases in crack growth rate and would therefore conclude that the *exponent*, *m*, is likely to be increased in materials of low static fracture toughness.

In Fig. 15 we have collected results from several authors on the variation of m with K_{IC} in quenched and tempered medium- and high-strength alloy steels.[5–7,35–38] Neglecting any influence of the differences in mean stress employed by these authors, which may lead to some of the scatter observed, it is clear that steep slopes ($m \geqslant 3$) occur almost entirely in steels of low toughness ($K_{IC} \leqslant 60$ $MNm^{-3/2}$).

Direct experimental support for the presence of static fracture components to explain the results shown in Fig. 15 can be found in two sets of observations.

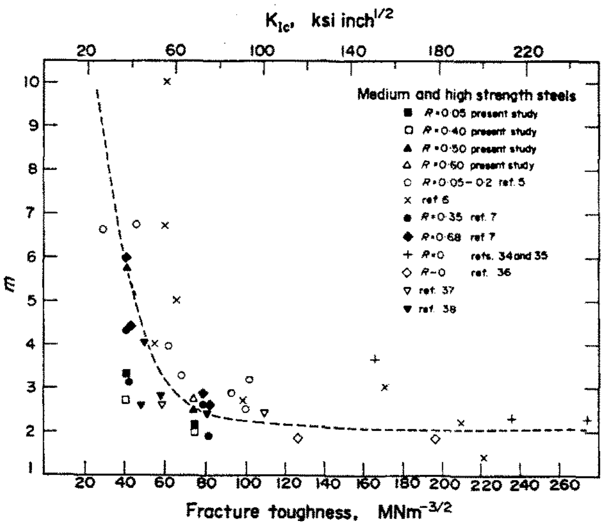

FIG. 15. Variation of the exponent 'm' from the Paris equation (1) with static fracture toughness K_{IC} for a number of medium- and high-strength steels.

If two separate papers published by Miller[5,39] are compared closely, it may be deduced that his very steep slopes ($m \sim 6$–7) were associated with a total "fatigue" fracture appearance consisting of a combination of intergranular fracture, fibrous rupture and quasi-cleavage, with little evidence of fatigue striations. For materials which yielded slopes of between 2 and 3, propagation was almost entirely by striation growth. Intermediate slopes were obtained where materials showed only isolated patches of striation growth, particularly at higher values of ΔK. Similarly the results published by Evans *et al.*[7] show that their high values of 'm' in low-toughness steels are associated with the presence of intergranular facets.

Additional support can be found from a comparison of the microscopic growth rates, determined from measurements of the striation spacings on the fracture surfaces, with the macroscopic growth rate, obtained from external measurements of the crack length. For several high strength steels[39] and low toughness aluminium alloys,[40,41] it has been found that the dependence on ΔK of the microscopic growth rate (S) is significantly less than that of the macroscopic growth rate (da/dN). The slope (m) of the growth-rate curve using values of S was found to be approximately 2, whereas that for da/dN was closer to 3. Such discrepancies can be readily explained if the macroscopic growth rate reflects the contribution from additional fracture modes.

We therefore conclude that the occurrence of brittle static fracture components during fatigue crack growth has two important consequences. Firstly, it produces a marked effect of mean stress on crack growth rate. Secondly, it can increase the apparent dependency of crack growth rate on ΔK, as given by the exponent 'm' in equation (1). Both these effects are likely to be associated with materials of low static toughness.

Accelerations of the fatigue growth rate in general may arise from cleavage, intergranular or fibrous fracture, and the occurrence of these under any particular testing conditions will be very much a characteristic of the material involved. For example, when cracking is accelerated by cleavage fracture, as in mild steel, it is possible to relate the critical value of K_{max} at which a burst occurs to the attainment of a critical level of tensile stress at a carbide particle situated at a grain boundary ahead of the crack tip.[30] For the intergranular fractures observed in the present work, the explanation of the critical K_{max} value for the major bursts is less clear. However, since recent evidence has shown that temper brittle intergranular fractures are growth controlled and critically dependent on the level of applied *tensile* stress,[14] it is not unreasonable to assume that the basic principles are similar to those associated with cleavage crack formation. The occurrence of segments of intergranular fracture at low stress intensities has been explained in terms of oxygen segregation in the grain boundaries,[42] constraint and restricted slip in the small plastic zone at low values of K_{max},[43] and environmental effects.[7,44] Since, for the unembrittled steel, isolated intergranular facets were not observed at stress intensities greater than 30 $MNm^{-3/2}$, it seems plausible that in this instance the restricted slip argument is most applicable. The onset of fibrous fracture during fatigue crack growth in high strength steels has been related to a critical value of the crack opening displacement range, by applying a critical strain criterion for crack growth.[45] However, the argument has not been developed to include any effects of K_{max}, and hence does not explain the influence of mean stress on the transition to fibrous growth.

The main point of the present paper, however, is that, even though the detailed reasons for the onset of static fracture modes may not be completely understood and need to be investigated further, the effects of such modes on the macroscopic "fatigue" crack growth rate are paramount.

CONCLUSIONS

The general conclusions on the nature of fatigue crack propagation in medium- to high-strength steels are summarised below:

(1) Evidence for the occurrence of monotonic or static modes of fracture (cleavage, intergranular and fibrous) during the conventional fatigue mechanism of striation growth has been presented.

(2) These additional fracture modes during fatigue growth are considered to be responsible for two general effects observed in fatigue crack propagation, namely, the occurrence of large dependencies of growth rate on the alternating stress intensity [i.e. large values of 'm' in equation (1)] and the marked influence of mean stress on the propagation rate. Both theoretical models and our own results indicate that such effects cannot be attributed to classical striation growth mechanisms.

(3) The effects are accentuated in thick sections and predominate in materials of low static fracture toughness.

ACKNOWLEDGEMENTS

Some preliminary experiments on this research were carried out by Mr G. Clark as part of an undergraduate research project. The authors would like to thank Mr Clark and Mr R. F. Smith for helpful discussions and experimental assistance, Professor R. W. K. Honeycombe for provision of laboratory facilities, and the Director of Computing Services, Cambridge University, for use of the TITAN computer. Financial support from the Science Research Council for one of the authors (R. O. R.) is gratefully acknowledged.

REFERENCES

1. P. C. PARIS, *Fatigue, an Interdisciplinary Approach* p. 107 Sagamore, New York (1964).
2. P. C. PARIS and F. ERDOGAN, *J. Basic Eng.* (Trans. ASME Series D) **85**, 528 (1963).
3. P. C. PARIS and R. P. WEI, ASM Symp. on Eng. Aspects of Fatigue, 1969 Mats. Engineering Congress, Philadelphia, Pa., (Oct. 1969).
4. R. E. JOHNSON, *ibid.*
5. G. A. MILLER, *Trans. ASM* **61**, 442 (1968).
6. W. G. CLARK and E. T. WESSEL, ASTM Special Technical Publication No. 463, 106 (1970).
7. P. R. V. EVANS, N. B. OWEN and B. E. HOPKINS. *Eng. Fract. Mech.* **3**, 463 (1971).
8. H. W. LIU, *J. Basic Eng.* (Trans. ASME Series D) **85**, 116 (1963).
9. K. R. LEHR and H. W. LIU, *Int. J. of Fracture Mech.* **5**, 45 (1969).
10. H. W. LIU and NOBU IINO, *Fracture* 1969, p. 812 Proc. 2nd Int. Conf. on Fracture", Brighton, (1969).
11. R. O. RITCHIE and J. F. KNOTT, Third International Conference on Fracture, Munich (1973).
12. T. C. LINDLEY and C. E. RICHARDS, *Effects of Second-Phase Particles on Mech. Prop. of Steel* p. 119, Proc. Conf. BSC/ISI Scarborough, (1971).
13. N. E. FROST, *J. Mech. Eng. Sci.* **4**, 22 (1962).
14. L. C. E. GENIETS, Ph.D. Thesis, University of Cambridge, (1971).
15. L. C. E. GENIETS and J. F. KNOTT, Presented at Inst. Metall./ISI Conf. on Grain Boundary Segregation, London. Nov. 1971. [summary *Met. Sci. J.* **6**, 69 (1972)].
16. D. F. STEIN and A. JOSHI, *ibid.* [summary *Met. Sci. J.* **6**, 67 (1972)].
17. G. CLARK, R. O. RITCHIE and J. F. KNOTT, *Nature–Physical Sciences*, **239**, 104 (1972).
18. P. F. CHAPMAN and L. C. E. GENIETS, to be published in *Phil. Mag.*
19. J. B. COHEN, A. HORLICK and M. JACOBSON, *Trans. ASM* **39**, 109 (1947).
20. R. O. RITCHIE, G. G. GARRETT and J. F. KNOTT, *Int. J. of Fracture Mech.* **7**, 462(1971).
21. R. O. RITCHIE, to be published, (available as Departmental Report).
22. W. F. BROWN and J. E. SRAWLEY, ASTM Special Technical Publication No. 410 (1966).
23. W. K. WILSON, *Eng. Fract. Mech.* **2**, 169 (1970).
24. W. F. BROWN and J. E. SRAWLEY, ASTM Special Technical Publication No. 463, 230 (1970).
25. C. LAIRD and C. G. SMITH, *Phil. Mag.* **7**, 847 (1962).
26. R. M. N. PELLOUX, *Trans. ASM* **62**, 281 (1969).
27. J. R. GRIFFITHS, I. L. MOGFORD and C. E. RICHARDS, *Met. Sci. J.* **5**, 150 (1971).
28. C. E. RICHARDS, Private communication (1972).
29. T. C. LINDLEY and C. E. RICHARDS, C.E.G.B. (Leatherhead) Laboratory Note No. RD/L/N 177/71 (1971).
30. R. O. RITCHIE, Ph.D. Thesis, University of Cambridge (1973).
31. C. M. HUDSON and J. T. SCARDINA, *Eng. Fract. Mech.* **1**, 429 (1969).
32. N. E. FROST, L. P. POOK and K. DENTON, *ibid.* **3**, 109 (1971).
33. S. PEARSON, *ibid.* **4**, 9 (1972).
34. T. W. CROOKER, L. A. COOLEY, E. A. LANGE and C. N. FREED, *Trans. ASM* **61**, 568 (1968).
35. T. W. CROOKER and E. A. LANGE, ASTM Special Technical Publication No. 462, 258 (1970).
36. R. C. BATES, W. G. CLARK and D. M. MOON, ASTM Special Technical Publication No. 453, 192 (1969).
37. R. P. WEI, P. M. TALDA and CHE-YU LI, ASTM Special Technical Publication No. 415, 460 (1967).
38. C. M. CARMAN and J. M. KATLIN, Paper No. 66–Met. 3, *J. Basic Eng.* (*Trans. ASME*), (1966).
39. G. A. MILLER, *Trans. ASM* **62**, 651 (1969).
40. R. M. N. PELLOUX, *ASM Trans. Quart.* **57**, 511 (1964).
41. J. KERSHAW and H. W. LIU, *Int. J. of Fracture Mech.* **7**, 269 (1971).
42. D. I. GOLLAND and R. L. JAMES, *Met. Sci. J.* **4**, 113 (1970).
43. G. BIRKBECK, A. E. INCKLE and G. W. J. WALDRON, *J. Mats. Sci.* **6**, 319 (1971).
44. E. P. DAHLBERG, *Trans. ASM* **58**, 46 (1965).
45. J. M. BARSOM, A.S.T.M. Special Technical Publication No. 486, 1 (1971).